ELSEVIER

Journal of Nuclear Materials 298 (2001) 19–26

journal of nuclear materials

www.elsevier.com/locate/jnucmat

A proposition for an improved theoretical treatment of the corrosion of multi-component glasses

R. Conradt [*]

Lehrstuhl für Glas und keramische Verbundwerkstoffe, Institut für Gesteinshüttenkunde, RWTH Aachen, Mauerstraße 5, 52064 Aachen, Germany

Abstract

The paper points out how the accumulated knowledge of glass corrosion and the latest understanding of the glassy state need to be merged in order to improve the predictive power of existing corrosion models. In specific, two areas are identified which require substantial improvement. These are, firstly, an adequate description of the effects of glass composition, and, secondly, an explicit formulation of the pH dependence of the forward reaction rate. The former problem is solved by employing a constitutional approach to the Gibbs energy of the glass. The latter problem is tackled by taking into account the occupation of the glass surface by charged species (H^+, OH^-, R^+, etc.). © 2001 Elsevier Science B.V. All rights reserved.

1. Introduction

For many years, the scientific community had felt quite comfortable with understanding and interpreting the interaction between glass and aqueous solution in terms of two distinct mechanisms, which are: network dissolution and leaching. It was only in the late 1970s that a larger number of scientists became active in the field, motivated by the global effort to establish a safe concept for the disposal of high level radioactive waste (HLW). It was at that time, too, that the scientific community realized how little they actually knew about glass corrosion. During the following years, a new understanding of glass corrosion emerged. Two of the most prominent milestones of this development are: a thermodynamic approach based on the ideas by Paul [1], and a general rate law of glass corrosion formulated by Grambow [2] in strict analogy to the ideas by Aargaard and Helgeson [3]. These concepts, however, did not reach the state of dissemination they deserved. Their impact on other areas of glass research remained comparatively small. Typical examples are: the recent discussion on the performance of table ware glass in dish washers; the development of highly resistant glasses for medical and industrial use; the biopersistance (in relation to a suspected cancerogenic potency) of inhaled man-made mineral fibres. Much of this work is based on empirical knowledge supported by the scientific concepts of the late 1970s. In Germany, for example, a so-called index of cancerogeneity KI [4] was adopted by legislation, reading

$$\mathrm{KI} = \mathrm{Na_2O} + \mathrm{K_2O} + \mathrm{B_2O_3} + \mathrm{CaO} + \mathrm{MgO} + \mathrm{BaO} - 2\mathrm{Al_2O_3} \tag{1}$$

(with oxide amounts given in wt%). According to this regulation, fibre compositions with $\mathrm{KI} > 40$ are classified as harmless, while the rest is considered as potentially harmful. The regulation ignores most of the hitherto understanding of glass corrosion. Yet, a communication gap is also found in the reverse direction. Scientists specialized in the field of glass corrosion seem to have taken little notice of the progress achieved in the description of the glassy state. As a consequence, some of the most powerful corrosion models suffer from an inadequate description of glass composition effects. It is the purpose of the present paper to point out how the knowledge of glass corrosion and the latest under-

---

[*] Tel.: +49-241 80 49 66; fax: +49-241 88 88 129.
E-mail address: conradt@ghi.rwth-aachen.de (R. Conradt).

0022-3115/01/$ - see front matter
PII: S0022-3115(01)00574-8

standing of the glassy state should be merged to improve the predictive power of corrosion models.

2. Adequate thermodynamic representation of glass composition

Until today, rate laws of the Aargaard–Helgeson–Grambow type [2,3] have been the most successful approach to glass corrosion. These rate laws are based on transition state theory and usually comprise the following three elements:

(A) A temperature and pH dependent forward rate for the rate controlling elementary step.

(B) A reaction turnover dependent Gibbs energy of hydration of the glass, ΔG_{hydr}, accounting for glass composition effects.

(C) The solubility product of the rate controlling species (for silicate glasses usually taken as SiO_2).

Point (A) is related to a local equilibrium instantaneously established at the interface between glass and aqueous solution. As Baucke [5–8] points out, this is a true thermodynamic equilibrium reflecting the composition of both the glass surface and the aqueous solution (in specific, the pH, pNa etc.). Knauss et al. [9] demonstrated for a five-component borosilicate glass that the forward rate is a function of pH as expected. The authors derived pH dependent rate constants which also reflected in some way the glass composition. Guy and Schott [10] developed a way to quantify the compositional dependence of the surface equilibrium by deriving – via a topological approach – a specification of surface sites even for multi-component glasses. In a similar way, considerable progress has been made with respect to point (C). The calculation of equilibria in aqueous systems is supported by an arsenal of sophisticated geochemical codes (e.g., [11,12]). However, as Advocat et al. [13] point out, there remains a major challenge for future development: The nature (and hence the solubility) of the amorphous silicia species is not constant but rather depends on the aqueous environment (including secondary solid precipitates) in which it is formed.

Comparatively little attention has been paid to point (B). The traditional ΔG_{hydr} approach does not seem so far to account for the effects of glass composition in an appropriate way. As explained below, this is mainly due to an inadequate approach to the thermodynamic state of the glass itself. In the classic thermodynamic approach to glass corrosion [1,14], the Gibbs energy of hydration ΔG_{hydr} of a glass is calculated from the weighted contributions of individual reactions like

$$Na_2SiO_3 + 2H^+ \rightarrow 2Na^+ + H_2SiO_3 \tag{2}$$

$$CaSiO_3 + 2H^+ \rightarrow Ca^{2+} + H_2SiO_3 \tag{3}$$

$$SiO_2 + 2H_2O \rightarrow H_2SiO_3 \tag{4}$$

$$Al_2O_3 + 3H_2O \rightarrow Al(OH)_3 \tag{5}$$

etc.

The ΔG_{hydr} values are calculated, based on tabulated standard data for vitreous SiO_2, amorphous or – depending on the scenario – crystalline $Al(OH)_3$; the rest is taken as crystalline phases or aqueous species, respectively. The individual contributions are weighted according to the stoichiometry of the glass involved. Now such a concept implies that the glass itself is a physical mixture of oxides and metasilicates, thus ignoring most of our understanding on glass structure and constitution. The consequences of this crude approach to glass composition soon became evident. For example, Perera and Doremus [15] did not find any predictive correspondence between measured dissolution rates and calculated Gibbs energies of hydration of a number of prominent industrial and natural glasses. A recent report [16] states that the ΔG_{hydr} approach to glass composition "has had limited success when dealing with the compositional range of real waste glasses. It was eventually dropped from the Grambow model and replaced with experimentally determined values for specific glass compositions". A recent review [17] points out in detail the difficulties in modeling glass composition effects, nevertheless, still recommends the use of ΔG_{hydr} values derived by the above approach. So, for the time being, the evaluation of equilibrium constants for glassy materials should be considered a turning point in kinetic modeling [13]. The difficulties involved in the description of oxide glasses stems from the fact that most of these glasses are extremely non-ideal mixtures of their oxide components. Additional information is needed to allow for the effects of mixing or, in other words, for the structural or configurational effects. Unfortunately, experimental data in this area are scant. Partial molar quantities of individual oxides are available for a number of binary, significantly less ternary, and very few quarternary systems only. In the following, a proposition is made on how to overcome these difficulties and to improve existing corrosion models in this specific area.

It has been shown [18,19] that glass composition is most adequately represented by a constitutional concept, i.e., in terms of its crystalline (equilibrium) reference state plus a (relatively small) energy of vitrification. This concept has been verified by numerous experiments, involving many experiments beyond the scope of – always slightly ambiguous and debatable – corrosion tests. As an example, Table 1 presents the compositions of three simple soda lime silicate glasses in terms of the amounts of: oxides, constitutional phases, oxides + metasilicates, and batch materials. Table 2 shows the heats of formation of these glasses from pure soda ash, limestone, and sand, as measured by high precision calorimetry [20], and as calculated. Experimental and calculated results deviate by less than 5% for

Table 1
Oxide composition, normative phase content, and batch composition of three simple soda lime silicate glasses

	Glass I	Glass II	Glass III
Glass composition in wt%			
Na_2O	13.0	15.2	15.8
CaO	11.7	13.8	10.1
SiO_2	75.3	71.0	74.1
Phase content in wt%			
(By constitutional phases)			
$Na_2O \cdot 2SiO_2$	–	3.6	–
$3Na_2O \cdot 8SiO_2$	–	–	16.4
$Na_2O \cdot CaO \cdot 5SiO_2$	87.4	90.6	75.6
$Na_2O \cdot 3CaO \cdot 6SiO_2$	0.1	5.8	–
SiO_2	12.5	–	8.0
(By metasilicates + oxides)			
$Na_2O \cdot SiO_2$	25.5	30.0	31.0
$CaO \cdot SiO_2$	24.3	28.6	21.0
SiO_2	50.2	41.4	48.0
Batch composition in wt%			
Soda ash	22.1	26.1	27.0
Limestone	20.9	24.6	18.1
Sand	75.3	71.0	74.1

Table 2
Heat of formation ΔH^f (in J/g glass) of three simple soda lime silicate glasses (compositions see Table 1) from soda ash, limestone, and quartz sand

	Glass I	Glass II	Glass III
By experiment:			
Direct calorimetry (J/g)	493	556	513
Solution calorimetry (J/g)	487	550	514
Mean value (J/g)	490	553	513
±Experimental error (%)	2	2	2
By calculation:			
Via constitutional phases (J/g)	508	563	537
Deviation (%)	4	2	4
Via metasilicates (J/g)	384	444	395
Deviation (%)	28	25	30

the constitutional approach, but more than 25% for the approach via oxides and metasilicates. By the same procedure, the heat demand of glass melting was calculated for 19 commercial raw material batches [21,22]. The results obtained by the constitutional approach matched with experimental data within ±4% (max. deviation found: 8% one outlier). Table 3 demonstrates again how accurate the constitutional approach works: Predicted oxide activities in glass melts agree with experimental values [23,24] well within the typical range of experimental error. Attention is also drawn to the work by Shakhmatkin et al. [25] demonstrating that glass properties can be predicted by a constitutional approach at a high accuracy. Thus we can be very confident that the constitutional approach correctly accounts for glass composition and also yields significantly approved values for ΔG_{hydr}.

3. Disentanglement of thermodynamic potentials involved in glass corrosion

In terms of thermodynamic states, the glass corrosion process at temperature T is presented by the sequence [26]

$$\text{glass } (T) + \text{aq. soln. } (T) \rightarrow \text{aq. species } (T). \tag{6}$$

Eq. (6) constitutes the Gibbs energy difference ΔG_{hydr}. From a formal point of view, we may rearrange this sequence as

$$\text{glass } (T) \rightarrow \text{aq. species } (T) - \text{aq. soln. } (T) \tag{7}$$

yielding the same difference ΔG_{hydr}. Now ΔG_{hydr} is a blend of data comprising the glass composition, the formation of glass and the formation of the aqueous solution, temperature dependencies, etc. These influences can be disentangled by interpreting Eq. (7) by the following sequence:

$$\text{glass } (T_0) \rightarrow \text{glass } (T) \tag{8a}$$

$$\text{c.r.s } (T_0) \rightarrow \text{glass } (T_0) \tag{8b}$$

$$\text{oxides } (T_0) \rightarrow \text{c.r.s. } (T_0) \tag{8c}$$

$$\text{oxides } (T_0) \rightarrow \text{aq. species } (T_0) - \text{aq. soln. } (T_0) \tag{8d}$$

$$\text{aq. species } (T_0) \rightarrow \text{aq. species } (T) \tag{8e}$$

$$\text{aq. soln. } (T_0) \rightarrow \text{aq. soln. } (T); \tag{8f}$$

c.r.s. = crystalline reference state; $T_0 = 298$ K. Thus, Eq. (7) is constituted by the following combination: (7) = (8d)+(8e)−(8f)−(8a)−(8b)−(8c). Note that each of the individual Eqs. (8a)–(8f) represents a well-defined unambiguous thermodynamic quantity denoting a standard energy of formation from the oxides (8c) and (8d), a standard energy of vitrification (8b), or a heat capacity term (8a, 8e and 8f), respectively. This disentanglement of the individual contributions contained in ΔG_{hydr} allows one to acquire the respective data without even thinking of a piece of glass being exposed to an aqueous solution. In specific, there is no need to collect any of these data from glass corrosion experiments (which is probably one of the least reliable sources). All data can be acquired by employing precision methods like calorimetry, emf measurements, potentiometry, etc. The remaining problem related to the sequence of Eqs. (8a)–(8f) is the constitutional problem, i.e., the determination of the c.r.s. for a given glass.

Table 3
Decadic logarithms of thermodynamic activities ($\log \boldsymbol{a}$) of individual oxides (bold print) in different glass melts; compositions given in mol%; $\log \boldsymbol{a}$ values determined by experiment [23,24], and calculated by the constitutional approach

Na_2O	CaO	Al_2O_3	SiO_2	Rest	T (K)	$\log \boldsymbol{a}$	
						Experiment	Calculation
25.0	0.0	5.0	70.0	0.0	1300	−9.5	−9.5
38.0	0.0	10.0	52.0	0.0	1300	−7.5	−7.6
0.0	**43.1**	26.4	30.5	0.0	1873	−1.6	−1.7
0.0	**38.9**	28.3	32.8	0.0	1873	−1.9	−1.9
0.0	**32.3**	31.4	36.3	0.0	1873	−2.3	−2.2
0.0	**25.2**	34.6	40.2	0.0	1873	−2.5	−2.7
14.0	9.0	2.0	72.0	3.0[a]	1300	−10.1	−10.4
14.0	9.0	2.0	72.0	3.0[a]	1350	−9.9	−10.1

[a] Float glass composition.

4. Determination of the crystalline reference state of a glassy material

A given oxide composition corresponds to a crystalline equilibrium state at 298 K, 1 bar, in an unambiguous way. This is true irrespective of the difficulties involved in identifying it. For binary, ternary and several quarternary systems, the c.r.s. can be directly read from existing phase diagrams. For multi-component systems, alternative strategies are required. The problem was first approached in geochemistry by the so-called C.I.P.W. calculation (see, e.g., [27]). The procedure yields normative mineral contents of igneous and metamorphic rocks from their overall composition. The results agree surprisingly well with the situation actually found in nature. Later [18], the principles of the C.I.P.W. calculation were refined and extended to man-made multi-component glasses: Instead of allotting, step by step, a fixed sequence of mineral phases (like in the original C.I.P.W. procedure), the predominant ternary or quarternary oxide system of a given glass composition is determined first. Then the constitutional phases of this particular system are adopted as a basis of a modified list of mineral phases, while the original list of phases is used for the minority oxides. This procedure generates – in agreement with the Gibbs phase rule – a list of phases k equal in number to the oxides j of the glass. Thus, the molar amounts n_k of the phases can be calculated from the glass composition by solving a simple linear equation system. Finally, the thermodynamic quantities $Z = G, H, S$, etc. of a glass are derived by

$$Z = \sum_k n_k \, Z_{k,\text{glassy}} \tag{9}$$

at an accuracy as reflected by the results in Tables 2 and 3 for $Z_{k,\text{glassy}}$, see [19,28]. Of course, the n_j and n_k must be referred to identical amounts of glass. For practical purposes, 100 g is taken in this paper, yielding Gibbs energies in the probably unfamiliar unit of kJ/100 g of glass. However, these figures are readily converted to kJ/mol of oxides by multiplication with $0.01 \cdot \Sigma x_j \cdot M_j$. Here, x_j and M_j denote the molar fraction and the molar mass of oxide j, respectively. Table 4 demonstrates the results for a mineral fibre glass (stone wool) and for the glass PNL-76-68. In both cases, the predominant oxide system covers more than 87 mol% of the entire glass composition, leaving little arbitrary choice for the determination of the c.r.s. The Gibbs energies of formation (from the elements) ΔG^f are −833.9 and −855.6 kJ/mol of oxides, respectively, which compares unfavorably to −846.5 and −858.5 kJ as derived via oxides and metasilicates. Very recent experimental results on the Gibbs energy of formation of a ternary borosilicate glass [29] showed similar deviations from the values calculated the traditional way. According to the sequence of Eqs. (8a)–(8f), any deviations in the ΔG^f of the glassy phase directly propagate to the predicted ΔG_{hydr} values. From this point of view, a constant bias δG for different glasses would be acceptable, and the traditional approach to ΔG_{hydr} could still be used for a comparative analysis of glass durability. As Table 5 shows, a small and nearly constant bias is found for simple soda lime glasses and for some HLW glasses. However, depending on the glass composition, the bias may reach quite large values. This is especially pronounced for glassy anorthite, disposite, albite, and devitrite and propagates to all glass types comprising the respective crystalline phases in their c.r.s.

5. Role of surface chemistry

Fig. 1(a) shows results [32] for two industrial mineral fibre compositions (so-called HT fibres with main components in wt%: 39–42 SiO_2, 20–21 Al_2O_3, 5–6 FeO, 7–8 MgO, 19–20 CaO). Calculated hydrolytic stabilities

Table 4

Oxide composition and crystalline reference system (c.r.s.) for a mineral fibre stone wool composition (Westerwaelder basalt), and for glass PNL-76-68, as calculated by a modified C.I.P.W. norm

Glass	Oxides j	Amount (g/100 g)	Phases k of the c.r.s.	Amount (g/100 g)
Stone wool	SiO_2[a]	45.10	$CaO \cdot MgO \cdot 2SiO_2$[a]	7.96
	TiO_2	2.69	$CaO \cdot TiO_2$	5.12
	Al_2O_3[a]	13.00	$CaO \cdot Al_2O_3 \cdot SiO_2$[a]	15.42
	Fe_2O_3	5.06	$FeO \cdot Fe_2O_3$	4.18
	FeO	6.52	$FeO \cdot SiO_2$	7.74
	Cr_2O_3	0.06	Cr_2O_3	0.05
	P_2O_5	0.95	$P_2O_5 \cdot 3CaO$	3.73
	MgO[a]	9.43	$2MgO \cdot SiO_2$[a]	48.51
	CaO[a]	10.80	$2CaO \cdot MgO \cdot 2SiO_2$[a]	3.28
	MnO	0.18	$MnO \cdot SiO_2$	0.55
	Na_2O	2.88	$Na_2O \cdot Al_2O_3 \cdot 6SiO_2$	12.67
	K_2O	1.36	$Na_2O \cdot Al_2O_3 \cdot 6SiO_2$	4.02
	Sum	98.02	Sum	98.02
PNL-76-68	SiO_2[a]	42.80	SiO_2[a]	24.63
	TiO_2	3.10	$CaO \cdot TiO_2$	5.28
	ZrO_2	1.70	$ZrO_2 \cdot SiO_2$	2.53
	Al_2O_3	0.5	$Na_2O \cdot Al_2O_3 \cdot 6SiO_2$	0.86
	B_2O_3[a]	8.5	$Na_2O \cdot B_2O_3$[a]	16.07
	Fe_2O_3[a]	10.80	Fe_2O_3[a]	10.80
	FeO	0.00	$FeO \cdot Fe_2O_3$	0.00
	CaO	2.20	$Na_2O \cdot 3CaO \cdot 6SiO_2$	0.08
	BaO	0.50	$Na2O \cdot Al_2O_3 \cdot SiO_2$	1.22
	ZnO	4.80	$2ZnO \cdot SiO_2$	6.57
	Na_2O[a]	15.00	$Na_2O \cdot 2SiO_2$[a]	21.52
	MoO_3	1.90	MoO_3	1.90
	Nd_2O_3	4.10	Nd_2O_3	4.10
	Cs_2O	0.80	$Cs_2O \cdot 2SiO_2$	1.14
	Sum	96.70	Sum	96.70

[a] Oxide or phase, respectively, of the predominant quarternary.

Table 5

Gibbs energies of formation from the elements ΔG^f for different glassy (gl) materials, given in kJ/mol of oxides; (a) calculated via c.r.s.; (b) calculated via an oxide + metasilicate speciation; δG is the deviation between both methods; the data for glassy anorthite, devitrite, albite, and devitrite in column (a) match well with tabulated literature data [30,31]

Glass type	M (g/mol)	ΔG^f (kJ/mol) (a)	ΔG^f (kJ/mol) (b)	δG (kJ/mol) (a)−(b)
Glass I	59.82	−799	−802	3
Glass II	59.77	−791	−794	3
Glass III	59.94	−794	−798	4
SRL-131	76.24	−949	−957	8
PNL-76-68	76.74	−856	−859	3
R7T7	71.08	−891	−893	2
Pyrex	62.03	−893	−888	−5
DGG-1	59.42	−793	−797	4
Stone wool	67.30	−834	−847	13
Anorthite (gl)	69.55	−989	−992	3
Diopside (gl)	54.14	−736	−753	17
Albite (gl)	65.56	−916	−910	−6
Devitrite (gl)	59.07	−784	−782	−2

in terms of ΔG_{hydr} and measured dissolution rates follow the same pattern. In other words, a relation like

$$\ln r = A + B \cdot \Delta G_{\mathrm{hydr}} \qquad (10)$$

with empirical constants A and B is valid. Such a relation is expected to hold, indeed, for a given corrosion test scenario with fixed experimental parameters

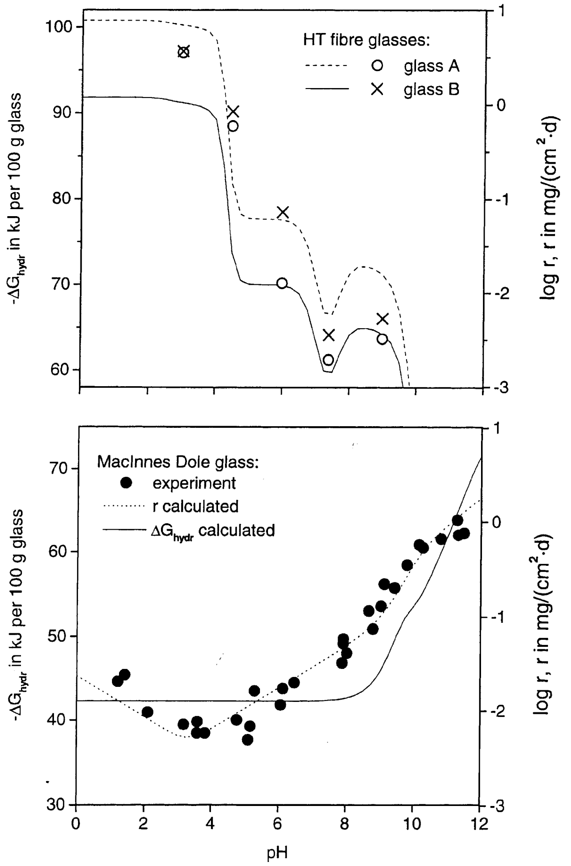

Fig. 1. Comparison of calculated ΔG_{hydr} values (solid and dashed lines) and calculated [34] rates (dotted line) to measured dissolution rates: (a) by [32]; (37 ± 1)°C, $SA/V = 0.06\ \mathrm{cm}^{-1}$, $c\,(\mathrm{NaCl}) = 0.154$ mol/l, soln. renewed in 7 d intervals; (b) by [33], 75°C, $SA/V = 0.67\ \mathrm{cm}^{-1}$, $c\,(\mathrm{NaCl}) = 0.2$ mol/l, initial rates.

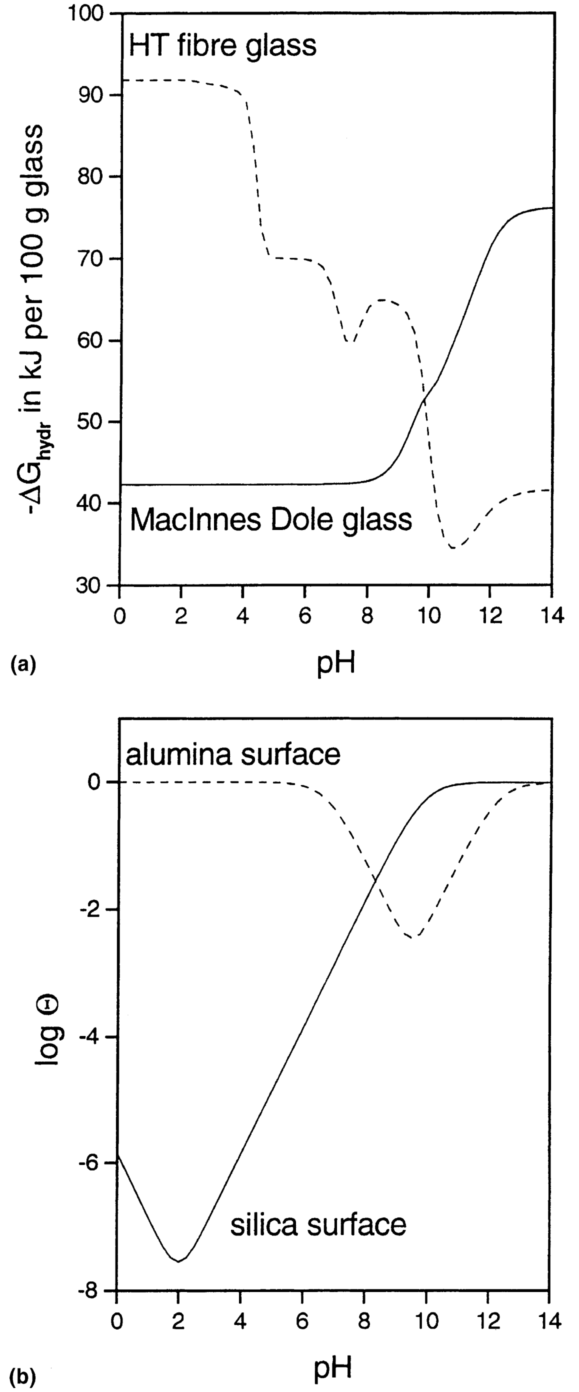

Fig. 2. Comparison of the pH dependence of ΔG_{hydr} (a) of a HT fibre glass and a MacInnes Dole glass to the pH dependence of the coverage of alumina and silica surfaces (b) by charged groups after [35,36].

[17]. For the investigated case, however, A and B show little or no pH dependence, which is an unexpected behavior reflecting little or no pH dependence of the forward reaction rate. By contrast, the series of experiments [33] on a silica rich glass (MacInnes Dole glass, 72 SiO_2, 6 CaO, 22 Na_2O by wt) shown in Fig. 1(b) displays the generally expected behavior with a pronounced pH dependence beyond the one already contained in ΔG_{hydr}. An interpretation of these observations is given in terms of the coverage of the glass surface by charged groups [10,24]. The coverage can be presented in terms of a Langmuir type surface coverage factor Θ,

$$\Theta \approx \sum_{\mathrm{j}} \frac{k_{\mathrm{j}} c_{\mathrm{j}}}{1 + k_{\mathrm{j}} \cdot c_{\mathrm{j}}}, \tag{11}$$

where k_{j} and c_{j} is the adsorption coefficient and concentration of the charged species j, respectively; $\mathrm{j} = \mathrm{H}^+$, OH^-, R^+, etc. As a consequence, the pH dependence of the corrosion rates r is determined by both ΔG_{hydr} and $\log \Theta$. Figs. 2(a)–(b) contrast the pH dependence of ΔG_{hydr} for an alumina rich HT fibre glass and the silica rich MacInnes Dole glass, respectively, to the surface coverage of alumina [35] and silica [36] surfaces. In fact, the combined effects of ΔG_{hydr} and $\log \Theta$ lead to a satisfactory interpretation of the pH dependence of the corrosion rates. For the silica rich glass, this is illustrated by the dotted line in Fig. 1(b). The comparatively weak pH dependence of $\log \Theta$ at the alumina surface provides an explanation for the predominance of the ΔG_{hydr} effect with the alumina rich glasses (Fig. 1(a)). The above examples demonstrate how the approach to ΔG_{hydr} proposed in this paper and an appropriate approach to surface charging (like [10]) should be combined.

6. Conclusion

The paper identifies two areas in which the otherwise very successful Grambow [2] type rate equations for glass corrosion need to be improved. The first area refers to the effects of glass composition. These effects should no longer be accounted for by the conventional thermodynamic approach describing the glass in terms of metasilicates and oxides, but rather by a new constitutional approach. This constitutional approach has been used to accurately predict compositional effects in several glass technological problems, comprising batch melting, evaporation from the melt, and glass corrosion. The second area refers to the pH dependence of the forward rate. The occupation of the glass surface by charged species (comprising H^+ and OH^-) is a key to this problem. It is a challenge for future work to merge both approaches into a single model. Such a model is expected not only to predict the effects of glass composition on the corrosion rates, but also to quantitatively describe the compositional changes (leaching) in the sub-surface zone of multi-component glasses.

References

[1] A. Paul, Chemistry of Glasses, Chapman and Hall, London, 1982.
[2] B. Grambow, in: D.E. Clark, B.K. Zoitos (Eds.), Corrosion of Glass, Ceramics, and Ceramic Superconductors, Noyes, NJ, 1992, p. 124.
[3] P. Aagaard, H.C. Helgeson, J. Am. Sci. 282 (1982) 237.
[4] Technical regulations for hazardous substances (German), Promulgation of BMA §52 (4) Gefahrstoffverordnung (TRGS 905), BArbBl (1994) no.6.
[5] F.G.K. Baucke, J. Non-Cryst. Solids 19 (1975) 75.
[6] F.G.K. Baucke, J. Non-Cryst. Solids 73 (1985) 215.
[7] F.G.K. Baucke, Fresenius J. Anal. Chem. 349 (1994) 582.
[8] F.G.K. Baucke, Ber. Bunsenges. Phys. Chem. 100 (1996) 1466.
[9] K.G. Knauss, W.L. Bourcier, K.D. McKeegan, C.I. Merzbacher, S.N. Nguyen, F.J. Ryerson, D.K. Smith, H.C. Weed, L. Newton, Mater. Res. Soc. Symp. Proc. 176 (1990) 371.
[10] C. Guy, J. Schott, Chem. Geol. 78 (1989) 181.
[11] T.J. Wolery, EQ3/6, a software package for geochemical modeling of aqueous systems, Lawrence Livermore National Laboratory, UCRL-MA-110662, 1992.
[12] D.L. Parkhurst, User's Guide to PHREEQC, a computer program for speciation, reaction path, advective-transport, and inverse geochemical calculations. US Geological Survey, Water-Resources Investigations Report 95-4227, Lakewood, Colorado, 1995.
[13] T. Advocat, J.L. Crovisier, B. Fritz, E. Vernaz, Mater. Res. Soc. Symp. Proc. 176 (1990) 241.
[14] C.M. Jantzen, in: D.E. Clark, B.K. Zoitos (Eds.), Corrosion of Glass, Ceramics, and Ceramic Superconductors, Noyes, NJ, 1992, p. 153.
[15] G. Perera, R.H. Doremus, J. Am. Ceram. Soc. 74 (1991) 1269.
[16] J. Sproull, W.L. Bourcier, B.P. McGrail, M.K. Altenhofen (Eds.), High-level Waste Borosilicate Glass: A Compendium of Corrosion Characteristics, vol. 1, Report no. DOE-EM-0177, U.S. Dept. of Energy, 1994.
[17] B. Grambow, in: R.W. Revie (Ed.), Uhlig's Corrosion Handbook, Wiley, London, 2000, p. 411.
[18] R. Conradt, in: H. Wendt (Ed.), Molten Salt Chemistry and Technology, vol. 5, TransTech, Zürich, 1998, p. 155.
[19] R. Conradt, in: H. Bach, D. Krause (Eds.), Analysis of the Composition and Structure of Glass and Glass Ceramics, Springer, Berlin, 1999, p. 232.
[20] C. Kröger, G. Kreitlow, Glastech. Ber. 29 (1956) 393.
[21] R. Conradt, P. Pimkhaokham, Glastech. Ber. 63K (1990) 134.
[22] C. Madivate, F. Müller, W. Wilsmann, Glastech. Ber. Glass Sci. Technol. 69 (1996) 167.
[23] M. Allibert et al., in: M. Allibert et al. (Eds.), The Slag Atlas, Verlag Stahleisen, Düsseldorf, 1995, p. 225.
[24] P. Sardjono, PhD thesis, Aachen, Germany, 1995.
[25] B.A. Shakhmatkin, N.M. Vedishcheva, M.M. Schultz, A.C. Wright, J. Non-Cryst. Solids 177 (1994) 249.
[26] R. Conradt, in: H. Bach, D. Krause (Eds.), Analysis of the Composition and Structure of Glass and Glass Ceramics, Springer, Berlin, 1999, p. 435.
[27] A.R. Philpotts, Principles of Ingneous and Metamorphic Petrology, Prentice-Hall, Englewood Cliffs, NJ, 1990.
[28] R. Conradt, in: D. Rammlmair et al. (Eds.), Applied Mineralogy, Balkema, Rotterdam, 1999, p. 115.
[29] Y. Linard, I. Yamashita, T. Atake, J. Rogez, P. Richet, J. Non-Cryst. Solids 286 (2001) 200.
[30] R.A. Robie, B.S. Hemingway, J.R. Fisher, Geol. Surv. Bull. 1452, U.S. Government Printing Office, Washington, 1978.
[31] V.I. Babushkin, G.M. Matveyev, O.P. Mchedlov-Petrossyan, Thermodynamics of Silicates, Springer, Berlin, 1985.
[32] S. Groß, U. Dahlmann, R. Conradt, in: Proceedings of the Fifth ESG Conference, Prague 1999, B1, p. 65.

[33] Z. Boksay, G. Bouquet, Phys. Chem. Glasses 21 (1980) 110.

[34] R. Conradt, P. Geasee, Ber. Bunsenges. Phys. Chem. 100 (1996) 1408.

[35] G. Sposito (Ed.), The Environmental Chemistry of Aluminum, CRC, Boca Raton, FL, 1996.

[36] R.K. Iler, The Chemistry of Silica, Wiley, New York, 1979.